GENETICS

Pervasive head-to-tail insertions of DNA templates mask desired CRISPR-Cas9–mediated genome editing events

Boris V. Skryabin[1]*, Delf-Magnus Kummerfeld[1], Leonid Gubar[1], Birte Seeger[1], Helena Kaiser[1], Anja Stegemann[1], Johannes Roth[2], Sven G. Meuth[3], Hermann Pavenstädt[4], Joanna Sherwood[5], Thomas Pap[5], Roland Wedlich-Söldner[6], Cord Sunderkötter[7], Yuri B. Schwartz[8], Juergen Brosius[9,10], Timofey S. Rozhdestvensky[1]*

CRISPR-Cas9–mediated homology-directed DNA repair is the method of choice for precise gene editing in a wide range of model organisms, including mouse and human. Broad use by the biomedical community refined the method, making it more efficient and sequence specific. Nevertheless, the rapidly evolving technique still contains pitfalls. During the generation of six different conditional knockout mouse models, we discovered that frequently (sometimes solely) homology-directed repair and/or nonhomologous end joining mechanisms caused multiple unwanted head-to-tail insertions of donor DNA templates. Disturbingly, conventionally applied PCR analysis, in most cases, failed to identify these multiple integration events, which led to a high rate of falsely claimed precisely edited alleles. We caution that comprehensive analysis of modified alleles is essential and offer practical solutions to correctly identify precisely edited chromosomes.

INTRODUCTION

Genome editing is a powerful research tool for biology and medicine. In recent years, considerable progress has been made in this area as a result of emerging new technologies that directly modify genes at the stage of single-cell embryos (zygote); stem cells, including induced pluripotent stem cells; or germ cells. The discovery and application of the following sequence-specific programmable nucleases exemplify some of the advances: (i) zinc finger nucleases (*1*), (ii) transcription activator–like effector nucleases (*2*), and (iii) CRISPR-Cas9 ribonucleoprotein complexes (*3*, *4*). CRISPR are short, prokaryotic, genomic, palindromic repeats located in clusters. These clusters are transcribed and processed into small RNAs (*5*) that interact with Cas9 proteins, resulting in a sequence-specific endonuclease (*6*). The CRISPR-Cas9 complex is composed of two RNA molecules: crRNA (CRISPR RNA) and tracrRNA (transactivator for crRNA) (*7*). The crRNA contains ~20 nt of recognition sequence complementary to the targeting region of DNA, whereas tracrRNA interacts with Cas9 protein and base pairs with crRNA (*8*). The minimal "artificial" CRISPR-Cas9 complex consists of a crRNA-tracrRNA molecule hybrid [guide RNA (gRNA)] and Cas9 protein–DNA endonuclease (*9*). Cas9 is a 1368–amino acid multidomain protein isolated from *Streptococcus pyogenes* (SpCas9). In conjunction with the crRNA-tracrRNA complex, Cas9 cleaves double-stranded DNA (dsDNA) adjusted to the PAM (protospacer adjacent motif; NGG sequence). The DNA strand complementary to crRNA (target strand) is cleaved by the HNH-like nuclease domain, and the opposite, nontarget strand is cleaved by the RuvC-like domain (*10*). The CRISPR-Cas9 complex has been broadly used to generate defined site-specific cleavage of genomic DNA; it is a fast, inexpensive, and effective DNA editing system that has a wide range of potential applications. In living cells, the sequence-specific dsDNA breaks are repaired by nonhomologous end joining (NHEJ) or homology-directed repair (HDR) mechanisms. NHEJ often results in small insertions or deletions at the dsDNA break site, which may impair the function of a targeted gene. The NHEJ mechanism is commonly used to generate conventional gene knockout models in a wide range of organisms. The HDR mechanism requires a specific donor DNA template, most often coinjected together with the CRISPR-Cas9 complex, and results in precise genome editing events. HDR enables the insertion of specific point mutations, the addition of in-frame translated epitopes, the performance of sequence-specific knock-in (KI) events of genes, the generation of conditional knockout (cKO) genetic models, etc. Once refined to perfection, CRISPR-Cas9–mediated HDR-based genome editing holds immense promise for gene therapy. Much of the genome editing community is invested in improving the efficiency and sequence specificity of the CRISPR-Cas9 complexes (*11*–*19*). However, several limitations of the technique, such as the low efficiency of HDR, off-target effects, and genomic rearrangements remain challenging obstacles (*20*, *21*).

Our study examines the generation of six cKO mouse models that used CRISPR-Cas9–mediated HDR mechanism in 10 KI procedures. A comprehensive analysis revealed that direct genome editing of zygotes had resulted in mosaic genotypes of targeted mice (F0 generation). Unexpectedly, more than half of the F1 offspring with modified loci displayed multiple head-to-tail donor DNA integrations. We demonstrated that both HDR and NHEJ mechanisms were used. Conventionally applied polymerase chain reaction (PCR) analyses using the outside targeting homology flanking primers

[1]Medical Faculty, Core Facility Transgenic Animal and Genetic Engineering Models (TRAM), University of Muenster, Muenster, Germany. [2]Institute of Immunology, University Hospital Muenster, Muenster, Germany. [3]Clinic of Neurology with Institute of Translational Neurology, University Hospital Muenster, Muenster, Germany. [4]Internal Medicine D, University Hospital Muenster, Muenster, Germany. [5]Institute of Experimental Musculoskeletal Medicine (IMM), University Hospital Muenster, Muenster, Germany. [6]Institute of Cell Dynamics and Imaging, University of Muenster, Muenster, Germany. [7]Department of Dermatology and Venereology, University Hospital Halle, Martin Luther University Halle-Wittenberg, Halle (Saale), Germany. [8]Department of Molecular Biology, Umeå University, 901 87 Umeå, Sweden. [9]Institute of Experimental Pathology (ZMBE), University of Muenster, Muenster, Germany. [10]Institutes for Systems Genetics, West China Hospital, Sichuan University, Chengdu 610041, China.
*Corresponding author. Email: skryabi@uni-muenster.de (B.V.S.); rozhdest@uni-muenster.de (T.S.R.)

erroneously displayed integration of the desired single copy template; thus, the analysis failed to identify insert multiplication. If undetected, then this would undermine the validity of studies involving these animal models. To avoid this shortcoming, we suggest methods that improve analyses and verification of correctly targeted loci.

RESULTS

Generation and analysis of F0 founders for cKO mouse models

The strategy to generate cKO mouse models by simultaneous CRISPR-Cas9–mediated insertions of two *LoxP* sites using two crRNA and two single-stranded oligodeoxynucleotides (ssODN) (2sgRNA-2ssODN), proposed by Yang *et al.* (*22*), has been shown to be inefficient in an extensive study involving more than 50 different genomic loci (*23*). Our alternative "one-step" strategy for the generation of cKO mouse models using CRISPR-Cas9 complexes and long donor DNA templates, containing two *LoxP* sites, is similar to those recently reported (*24*–*26*) and could be demonstrated by *S100a8* (calcium-binding protein A8) gene targeting. On the basis of computational analysis, we predicted that genomic elimination of the second exon would result in a translational frameshift leading to *S100a8* gene inactivation. Therefore, we designed a donor DNA fragment with *LoxP* sites flanking the second

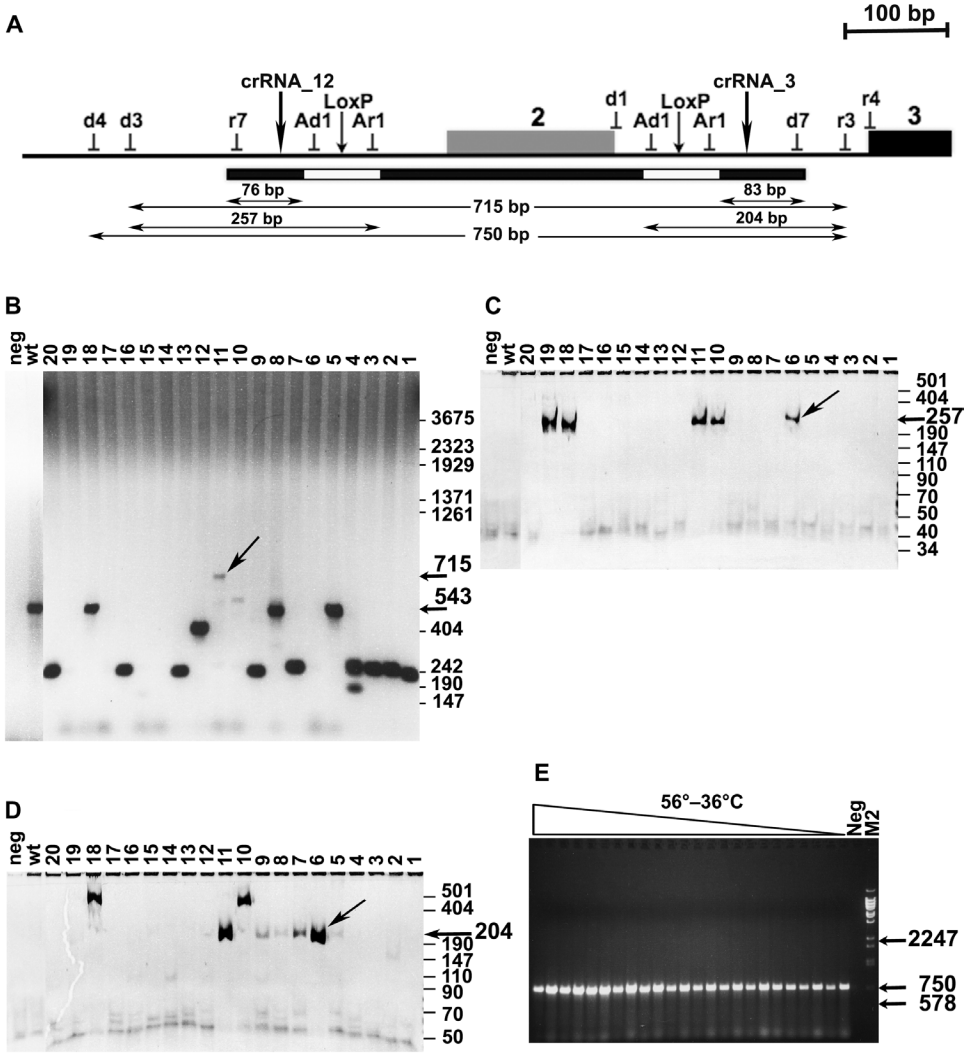

Fig. 1. PCR analysis of the *S100a8* targeted locus. (**A**) Genomic structure of the targeted locus with positions of PCR primers (d1, d3, d4, d7, r3, r4, and r7). Intronic regions are represented as lines, and exons are represented as filled boxes numbered above. The oligonucleotide pairs Ad1 and Ar1 are not present in the mouse genome but introduced as diagnostic sequences together with the *LoxP* sites. The black bar below is the schematic representation of the donor DNA template; *LoxP* sites are represented as white boxes. Sizes of homology arms and PCR products obtained with different primer combinations on (B) to (E) are indicated. (**B**) PCR analysis of genomic DNA from F0 founder mice 1 to 20 (labeled above) using primer pair d3/r3 located outside of the DNA template homology arms (A). The PCR products of 715 and 543 bp correspond to the correctly targeted (founder 11 labeled by an arrow) and wild-type (animals 5, 8, 10, and 18) alleles of the *S100a8* gene, respectively. The PCR products (>715 bp) presumably originating from multiple head-to-tail integrations of the DNA template were not detected. Size marker positions (in base pairs) are shown on the right. (**C** and **D**) PCR analyses of DNA samples from F0 founder mice 1 to 20 using primer pairs d3/Ar1 (C) and Ad1/r3 (D). (C) The PCR product of 257 bp corresponds to HDR integration of the 5′ homology arm detected in mouse samples 6 (labeled by arrow), 10, 11, 18, and 19. (D) The expected PCR product of 204 bp was detected in animals 6 (labeled by arrow), 7 to 9, and 11. In mouse numbers 10 and 18, the 3′ end of the DNA template integrated via NHEJ mechanism. (B to D) Genomic DNA from wild-type C57BL/6J mouse (wt) and water (neg) were used as controls. (**E**) PCR analysis at different annealing temperatures of genomic DNA from F0 founder number 6 using primer pair d4/r3. Only one PCR product of 750 bp, corresponding to a single copy targeted locus, was detected. A predicted PCR product for multiple head-to-tail DNA template amplification (~2247 bp) was not detected.

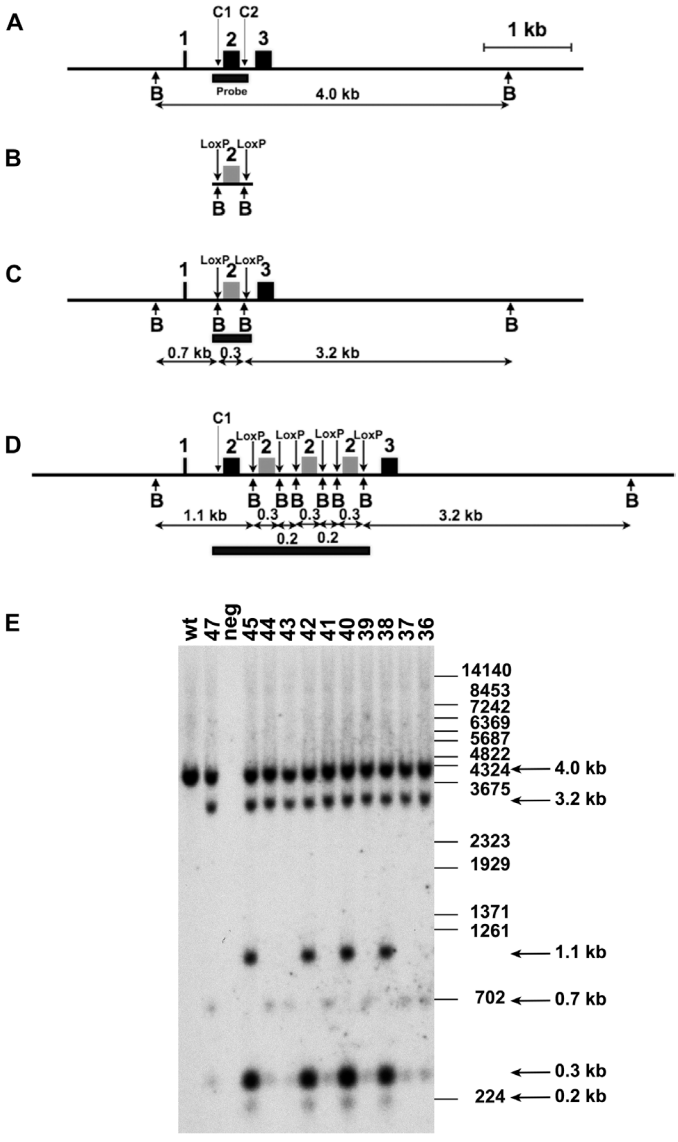

Fig. 2. Schematic representation of the *S100a8* gene targeting strategy. (**A**) Wild-type mouse *S100a8* locus. Exon 2 was chosen for elimination. Intronic and intergenic regions are represented as lines, and exons are represented as filled boxes numbered above. The vertical arrows indicate the target sites for the CRISPR-Cas9 complex with crRNA12 (C1) and crRNA3 (C2). The arrows marked with "B" correspond to Bam HI restriction endonuclease sites. The black bars below [marked "probe" in (A)] correspond to areas recognized by donor DNA–specific probes used in Southern blot analyses. The horizontal arrows denote the expected sizes of restriction DNA fragments given in kilobase. (**B**) Donor DNA template used in this study; the two *LoxP* sites are indicated by vertical arrows. (**C**) Genomic locus after HDR with single copy integration. (**D**) Targeted genomic locus with triple insertion of the donor DNA template. (**E**) Southern blot analysis of genomic DNA of the F1 offspring (36 to 45 and 47) hybridized with the template-specific probe [indicated in (A)]. Bam HI enzymatic digestion revealed the wild-type allele (4.0 kb) and three DNA fragments (3.2, 0.7, and 0.3 kb) corresponding to the targeted allele [marked in (C)]. DNA samples 36, 37, 39, 41, 43, 44, and 47 contain the correctly targeted *S100a8* allele (*S100a8*$^{+/-}$). Samples 38, 40, 42, and 45 contain DNA fragments of 1.1 and 0.2 kb in size, indicating multiple copy head-to-tail integrations at the targeted locus [marked in (D)]. Size marker positions (in base pairs) are shown on the right. The DNA sample from the wild-type control mouse is indicated as "wt."

exon of *S100a8* gene (Figs. 1A and 2, A to D). Our general strategy for one-step insertion of both *LoxP* sites relied on the active cellular HDR mechanism. We constructed a DNA template harboring exon-intronic regions flanked by *LoxP* sites with relatively short (76/83 nt) PAM-mutated homology arms (Figs. 1A and 2B). To select CRISPR-Cas9 complexes that efficiently cut genomic DNA at a chosen position, we designed at least three sequence-specific crRNAs for each flanking region. To gauge whether selected crRNA pairs efficiently guide genomic deletion in vivo, we injected Cas9 components with different combinations of crRNAs into fertilized mouse oocytes. Subsequent PCR amplification of loci between pairs of crRNAs determined the efficiency of CRISPR-Cas9 complex targeting (fig. S1). The most efficient crRNA pair as well as the donor DNA template and Cas9 components were then microinjected into the cytoplasm of fertilized mouse oocytes (tables S1 and S2). For the *S100a8* project, we obtained 34 pups (F0 generation) from 193 modified embryos. Initially, the selection of positively targeted mice was performed by PCR amplification of the genomic DNA region with d3 and r3 primers located outside the donor DNA flanking homology region (Fig. 1, A and B). We detected appropriate [~700 base pairs (bp)] PCR products representing a potentially desired targeted locus for mouse number 11 only (Fig. 1B). The other animals contained either wild type (~550 bp) or deletions surrounding the targeted *S100a8* exon-intronic region (Fig. 1B). The infrequent HDR events in combination with negative amplification results for most of the animals prompted us to investigate all mice with a different PCR approach; thus, we decided to amplify sequences adjacent to the *LoxP* sites paired with primers located in the corresponding genomic flanks. We used PCR primers d3/Ar1 and Ad1/r3 for the 5′ and 3′ regions, respectively, as shown in Fig. 1 (A, C, and D). Founder (F0) number 11 was confirmed to contain the correctly targeted allele, but an additional founder (number 6) was positively identified (Fig. 1, C and D). Notably, six mice that were previously identified as harboring only wild-type alleles or deletions within the targeted region revealed the presence of at least one potentially HDR-integrated *LoxP* site (Fig. 1, C and D). To exclude false-positive PCR identification of founder number 6, we performed gradient PCR amplification of donor DNA together with flanking regions using a combination of either d4/r4 or d4/r3 primers (Fig. 1, A and E, and fig. S2). In both amplification schemes, only a single PCR product was detected, suggesting correct HDR integration of a single copy donor DNA template (Fig. 1E and fig. S2).

Analysis of F1 generation mice revealed mosaicism of F0 founders

The offspring obtained after crossing *S100a8* cKO founder number 6 with wild-type mice was further analyzed by PCR and sequencing. Unexpectedly, we detected two types of locus targeting. In the first, we confirmed the correct CRISPR-Cas9 nuclease C1 and C2 cleavage of the genomic DNA locus and single copy integration of donor DNA template via HDR mechanism in offspring numbers 36, 37, 39, 41, 43, 44, and 47 (Fig. 2, C and E). The correct integration at the nucleotide level was confirmed by sequencing. The second type corresponded to tandemly multiplied DNA template integration yielding up to three copies [confirmed by quantitative PCR and digital droplet PCR analyses (see the Supplementary Materials)] in a head-to-tail configuration at a single CRISPR-Cas9 nuclease C2–mediated DNA break (Figs. 2, D and E, and 3 and fig. S3). In these cases, the 3′-ends of the DNA fragments integrated via HDR, while the

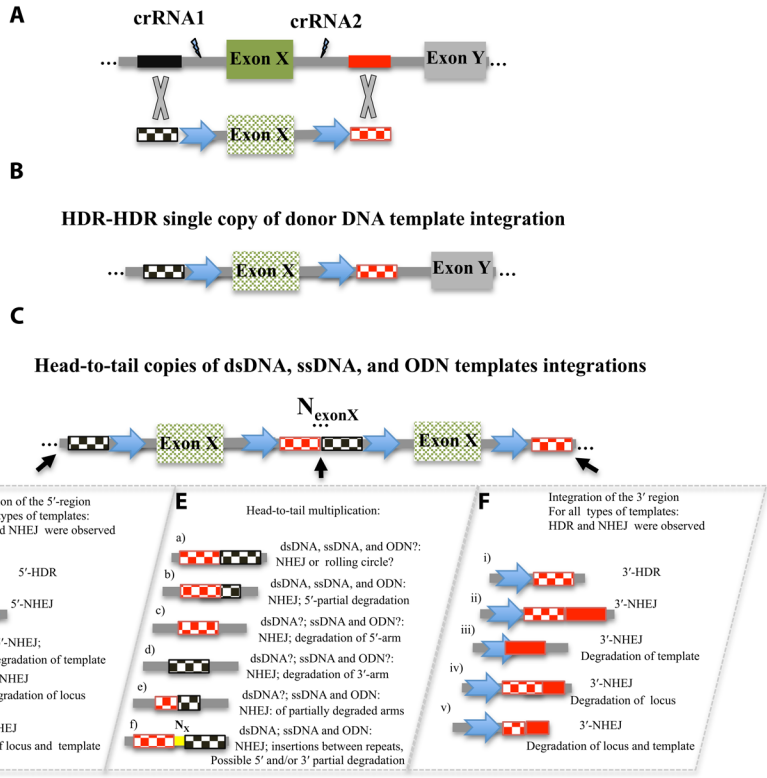

Fig. 3. Different types and mechanisms of donor DNA integrations and multiplications. (**A**) Schematic representation of the loci for the cKO targeting strategy. Intronic regions are represented by gray lines, original exons are represented by filled boxes, exon X of donor DNA template is indicated as patterned boxes. Homology arms for HDR in the targeted locus are marked as black and red lines for left and right flanks, respectively. For better visualization, the respective homology arms of the donor DNA template are indicated by chess pattern. The target sites of the CRISPR-Cas9 complex are denoted as crRNA1 and crRNA2. (**B**) Integration of a single donor DNA template using HDR mechanism is shown. (**C**) Head-to-tail integration of donor DNA template is schematically drawn. (**D** and **F**) Different types of 5′ (D) and 3′ (F) integration events that were confirmed by sequencing are indicated. (**E**) Different types of observed repeat junctions of multiplied dsDNA and ssDNAs donor DNA templates are indicated. In addition, we analyzed the sequence of repeat junctions during head-to-tail multiplications of single stranded oligodeoxynucleotides (ODN, in *Il4* locus, data not shown). Question mark (?) denotes a predicted but not experimentally verified scenario for dsDNA or ODN donors. (**E a**) We could not completely exclude that a rolling cycle mechanism for dsDNA or ssDNA multiplication could be responsible for at least part of the multimers where all ligated junctions are identical (cases from *S100a8* and *Treck1* loci). However, for a number of analyzed dsDNA-, ssDNA-, or ODN-derived head-to-tail repeats in the F1 generation, we identified various sequencing patterns within junction sites in each of the analyzed animals (**E b-e**). In a few cases, insertions of foreign DNA were observed at the junction sites between repeats (**E f**). Notably, head-to-head or tail-to-tail template multiplication was not observed. However, small inverted repeats originating from donor templates were observed within junction sites between head-to-tail repeats. This observation suggests that head-to-head or tail-to-tail ligations of DNA templates occur but are not stable in the locus and deleted (as inverted repeats) during cell division. In summary, obtained data indicate that NHEJ could be the major mechanism responsible for head-to-tail donor DNA multimerization.

5′-ends integrated via an NHEJ mechanism (Fig. 3 and fig. S3). As discussed in detail below, head-to-tail multiplications of donor DNA are not unique for *S100a8* and were detected in eight additional KI projects involving six different gene loci (Table 1 and figs. S4 to S7).

PCR analysis of animals with multiple head-to-tail DNA template integration

As previously mentioned, PCR analysis of F0 animals using primers flanking homology arms of DNA inserts did not reveal the presence of multiple tandem duplications in the targeted locus at various PCR amplification parameters; this includes different primers, as well as various touchdown and annealing temperatures (Fig. 1E and fig. S2). For all other one-step cKO projects, we only detected amplification products indicating "single copy insertion" (fig. S4C).

Considering difficulties in identifying head-to-tail insertions when relatively long donor templates were used (from 550 bp to 1.65 kb), we tested the HDR-mediated integration of a single-stranded DNA (ssDNA) harboring one *LoxP* site (~210 nt) during the construction of an *Il4* gene conditional mouse model (Fig. 4A). Multiple head-to-tail integrations of a single *LoxP* site were verified in the F1 mouse offspring. A total of 49 mice were PCR-analyzed using primers (SD1 and SR1) flanking the *LoxP* site in the homology arms (Fig. 4A). Tandem multiplication of the *LoxP*-harboring DNA template was detected in five mice: numbers 34, 40, 42, 44, and 48; all other mice revealed a PCR product corresponding to a single copy *LoxP* integration into the *Il4* gene locus using the HDR-HDR mechanism (Fig. 4B). This relatively low frequency of head-to-tail amplification was suspicious. Hence, we developed and performed additional control PCR amplification by using nonoverlapping bidirectional primers (SD1r and SR1d) that would specifically detect head-to-tail *LoxP* repeats (Fig. 4C). Unexpectedly, a total of 30 mice containing multiple copies of donor DNA were detected, indicating that ~83% of mice harboring *LoxP* head-to-tail multiplications were not verified by standard, commonly used PCR detection methods (Fig. 4, C and D).

Table 1. Summary of cKO loci targeting and mechanisms of donor DNA integrations. Gene name, the names for cKO-targeted genes are indicated [official ID provided by MGI (Mouse Genome Informatics)]; No. of F0 selected animals, number of F0 founders selected to contain a positively targeted allele; No. of F1 analyzed animals, number of analyzed mice from the F1 generation; No. of F1 positive SC animals, number of mice with correct HDR-HDR single copy donor template integration; No. of F1 positive MC animals, number of mice with identified multiple integrated copies of donor template; (F0), multiple copy integration of donor DNA template was identified in F0 founders; template size/strandedness (ss-ds DNA), donor DNA template sizes and strandedness are indicated; mechanism, mechanism for donor DNA template integration as determined; nd - not determined.

Gene name	No. of F0 selected animals	No. of F1 analyzed animals	No. of F1 positive SC animals	No. of F1 positive MC animals	Template size/ strandedness (ss-ds DNA)	Mechanism
S100a8	2	14 (**No.6**) 7 (**No.11**)	9 (**No.6**) 4 (**No.11**)	5 3	ssDNA (PCR) **591 nt**	**HDR-HDR** **NHEJ-HDR** **NHEJ-NHEJ**
Trek1	2	21	0	16	dsDNA **1257 bp**	**HDR-NHEJ** **NHEJ-HDR**
Trek1	6	28	0	12	ssDNA (PCR), **1257 nt**	**HDR-HDR**, **NHEJ-HDR**, **HDR-NHEJ**
Trek1	3	26	0	3(F0)	ssDNA (IDT) **1286 nt**	**nd**
Inf2	11	34	2	15	ssDNA (PCR) **711 nt**	**HDR-HDR**
Trpc6	3	22	5	nd	dsDNA **880 bp**	**HDR-HDR**
Trpc6	4	34	5	2	ssDNA (PCR) **880 nt**	**HDR-HDR**
Ccnd2	1	46	19	1(F0)	dsDNA **1658 bp**	**HDR-HDR**
Il4_5'LoxP	18	49	19	30	ssDNA (PCR) **210 bp**	**HDR-HDR**
Il4_flox	4	41	0	1(F0)	ssDNA (PCR) **1258 nt**	**NHEJ-HDR**
			Total F1: 63 (~43%)	Total F1: 83 (~57%)		

Southern blot analysis of targeted genomic loci

Alerted by the high false-positive rate of conventional PCR analysis, we turned to Southern blot hybridization to test the frequency of multiple head-to-tail integrations. Southern blot hybridization analyses characterized locus-specific targeting of the following mouse gene loci: *S100a8*, *Trek1*, *Inf2*, *Trpc6*, and *Ccnd2* (Fig. 2E and figs. S4 to S7). In all cases, ^{32}P-labeled donor DNA templates were used as a specific probe for hybridization (table S2). To facilitate the correct detection of single copy integrations, we incorporated additional restriction endonuclease recognition sites adjacent to the introduced *LoxP* sequences (Fig. 2B and figs. S4 to S7A). Restriction endonuclease recognition sites were chosen depending on the presence of the same sites in the targeted locus, assuming that following genomic DNA digestion, the resulting fragments would be unambiguously identifiable by size during electrophoresis in 0.8% agarose gels. For example, in the chosen region of the *S100a8* conditionally targeted locus, the flanking Bam HI endonuclease sites were located 4 kb apart in the wild-type allele (Fig. 2A). Complete digestion of genomic DNA of the correctly targeted locus should reveal 3.2-, 0.7-, and 0.3-kb DNA fragments (Fig. 2C), while the observed 1.1- and 0.2-kb fragments indicated multiple head-to-tail integrations of donor DNA via the NHEJ-HDR mechanisms (Fig. 2D). Using this strategy, we could clearly identify multiple copy integrations of donor DNA template during the generation of cKO mouse models, both in F0 and F1 offspring (Table 1, Fig. 2E, and figs. S4 to S7). Our analyses also revealed that multiple head-to-tail donor DNA template integrations arose via HDR-NHEJ, HDR-HDR, or NHEJ-NHEJ mechanisms (Table 1, Fig. 3, and figs. S4 to S7). Overall, we conclude that the repetitive head-to-tail integration of the donor DNA template is a common by-product of the CRISPR-Cas9–mediated HDR-based genome editing process, regardless of the donor DNA template size, sequence composition, or strandedness of the template (dsDNA or ssDNA) (Table 1). Southern blot hybridization analysis enabled the identification of single copy, positively targeted mice already in the F0 generation (fig. S7 and Table 1). However, because of the mosaic nature of donor DNA integration for some of the F0 mice, which indicated multiple copy integrations, we were, after crossing, able to identify offspring that harbored the desired single copy targeted allele.

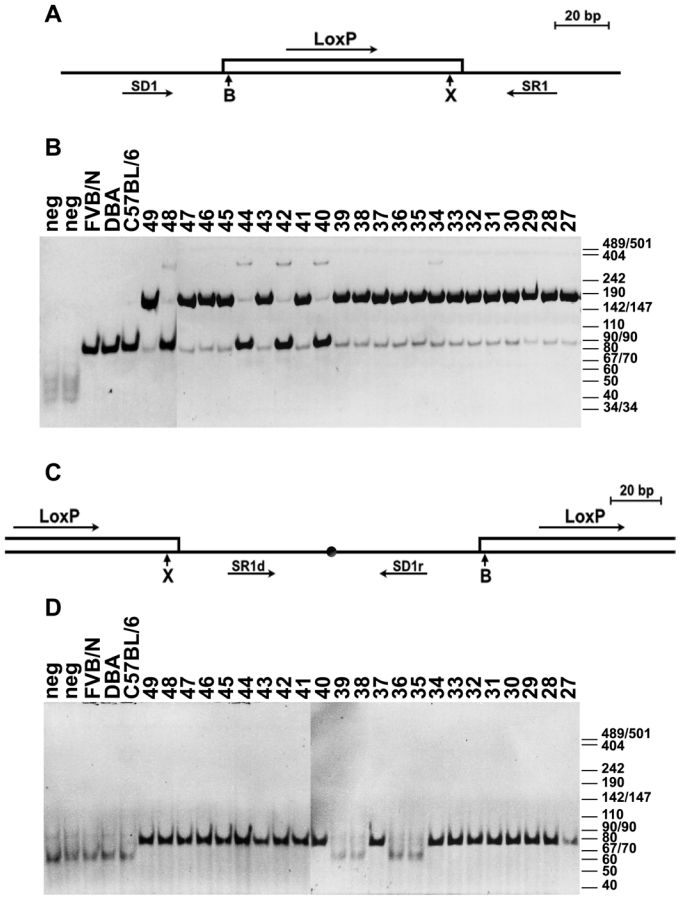

Fig. 4. Analysis of F1 mice for *LoxP* site integration in the *Il4* locus. (**A**) Schematic representation of the *Il4* 5′-*LoxP* DNA template. The genomic region is represented by lines, and the inserted artificial DNA sequence is indicated by an open rectangle. The 5′-*LoxP* site is designated by an arrow above, and the restriction endonuclease sites Bam HI (B) and Xho I (X) are indicated below. PCR primers are denoted by arrows. (**B**) PCR analysis of genomic DNA from selected F1 founder mice using the SD1/SR1 primer pair. (**C**) Schematic representation of a bidirectional primer strategy used to detect head-to-tail multiplication of donor DNA template. PCR primers are denoted by arrows, the repeat junction site is indicated by a black circle. (**D**) PCR analysis of genomic DNA from selected F1 founder mice using bidirectional primers SD1r and SR1d specifically detecting head-to-tail *LoxP* target DNA repeats.

DISCUSSION

CRISPR-Cas9 endonuclease has rapidly emerged as a state-of-the-art tool for genome editing in model organisms from all kingdoms of life (*27*). From the assembly of the CRISPR-Cas9 complex and the discovery of direct targeting of specific genomic sequences in vitro (*9*, *28*), it took only 6 months to experimentally verify in vitro findings in bacterial and mammalian cells (*3*, *4*, *29*). The establishment of genetically modified mouse models to study the potential functional roles of genes and their products in human diseases is an important aspect of biomedical studies (*30*–*34*). cKO mouse models constitute a powerful approach that enables the investigation of gene functions in specific cell types and/or in a development-specific manner (*35*, *36*).

Nevertheless, our study uncovered serious pitfalls exemplified in 10 separate KI procedures during the construction of six cKO mouse models that need to be taken into account. All gene-targeting protocols were performed by direct injection of CRISPR-Cas9 components together with donor DNA template into fertilized oocytes. Eight KIs were performed with relatively long donor DNA fragments (~700 to 1650 nt). Seven procedures used ssDNA and three dsDNA templates (Table 1). Three KI attempts with ssDNA and one with dsDNA templates did not yield the intended single copy integration of donor template (Table 1).

Efficiencies of donor DNA integration were variable and correlated with template size; in general, longer templates integrated less efficiently (Table 1). We noticed that most edited mice obtained from CRISPR-Cas9–modified zygotes (F0 generation) exhibited mosaic genotypes, harboring subpopulations of cells derived from different DNA integration events, and contained diverse copy numbers in the targeted loci. Our data suggest that PCR amplification of short genomic flanking regions in conjunction with inserted donor DNA is the most efficient and reliable approach for the identification of F0 mice with correctly targeted loci. Positive PCR results on both flanks indicated that a certain subpopulation of cells contains HDR-integrated DNA template (Fig. 1, C and D). However, longer PCR products representing subpopulations of cells with target DNA integrated via HDR-NHEJ or NHEJ-NHEJ are difficult to amplify. Nevertheless, in some cases, most probably depending on the degree of mosaicism and PCR primer locations, these arrangements could be detected as well (Fig. 1D, numbers 10 and 18).

When the selected F0 founders were crossed with wild-type mice for F1 offspring production, we often detected animals harboring multiple head-to-tail integrations of the donor template at the targeted loci (Fig. 3). We observed template multiplication irrespective of size, nucleotide composition, or the utilization of dsDNA or ssDNA (Table 1). A commonly applied PCR verification method in heterozygotic animals using template-specific primers in most cases erroneously identified those as single copy integration events. Moreover, in cases of multiple-copy HDR-HDR–based integrations of donor DNA, it proved impossible to correctly identify the desired single copy mice by amplification with primers set in the genomic flanking regions followed by PCR product sequencing.

To correct this error, we propose methods that can be used for the successful identification of HDR-HDR–based single copy targeted mouse loci. The first approach is based on a combination of PCR analyses: F0 and F1 founders harboring an HDR-HDR–based insertion of donor DNA could be identified using PCR amplification of flanking regions including elements of the insert (Fig. 1, C and D). A repeated head-to-tail template could be detected by a second PCR step using bidirectional, nonoverlapping primers (Fig. 4C). Furthermore, candidates for singly targeted loci should be sequenced to confirm the absence of possible mutations in the inserted donor DNA template. This relatively simple strategy could be useful for verification of any genome KI models, including point mutations in genes, specific deletions, or insertions in all species. Notably, identification of F0 founders with positive PCR results on both flanks does not guarantee that offspring will contain the correctly targeted single copy locus. On the other hand, identification of single copy positively targeted mice in the F0 generation is relatively rare. Since the mosaic nature of donor DNA integration often results in subpopulations of germ cells with correctly targeted loci, we therefore recommend crossing F0 candidates displaying HDR-HDR–integrated donor DNA template with wild-type animals and to perform a second PCR step using bidirectional, nonoverlapping primers on F1 offspring.

As shown in this study, Southern blot analysis is an additional method to reliably identify intended F1 founders. Below, we outline a strategy to design donor templates that permits the unambiguous identification of single copy targeted loci. We recommend the incorporation of two specific restriction endonuclease sites flanking the *LoxP* regions. This will allow the detection of small DNA fragments on Southern blots in the event that multiple donor template copies are integrated (Fig. 2E and figs. S4 to S7). Notably, the fragments should not be too small, as Southern blots poorly detect small size DNA fragments; this is illustrated by the failure to expose the 0.2-kb signal in the *Trpc6* gene cKO project (fig. S6C).

Despite the advantages of CRISPR-Cas9–based genome editing, a number of potential problems such as target specificity and off-target effects still impede the CRISPR-Cas9 technology for use in biomedical research; further efforts are necessary to overcome these hurdles. Our study examines problems that are not unique for the CRISPR-Cas9 system but instead generally affect direct KI genome targeting. In multiple cases, we documented that the insertion of donor DNA via the HDR mechanism results in mosaicism yielding subpopulations of cells with head-to-tail template amplification in the modified loci. Our findings and strategies are important elements that will aid in unlocking the full potential of the CRISPR-Cas9–mediated genome editing protocols for the generation of custom-designed gene variants for biomedical research and gene therapy.

MATERIALS AND METHODS

Cytoplasmic microinjections of the CRISPR-Cas9 components into fertilized oocytes

For the preparation of CRISPR-Cas9 microinjection solution, commercially synthesized crRNA (table S1), tracrRNA and, Cas9 protein [Integrated DNA Technologies (IDT), USA] were mixed as follows: 100 pmol of crRNA were mixed with 100 pmol of tracrRNA (when two crRNAs were used, the concentration of tracrRNA was increased to 200 pmol) in 10 mM potassium acetate and 3 mM Hepes (pH 7.5) buffer and incubated at 95°C for 2 min, followed by cooling to room temperature. The annealed crRNA/tracrRNA complex was mixed with Cas9 mRNA, Cas9 protein, and DNA target fragment. The final concentrations of CRISPR-Cas9 components in 0.6 mM Hepes (pH 7.5) and 2 mM potassium acetate microinjection buffer were as follows: crRNA (2 pmol/μl), tracrRNA (2 pmol/μl) (or 4 pmol/μl of tracrRNA if two crRNAs were used), Cas9 mRNA (10 ng/μl), Cas9 protein (25 ng/μl), and DNA target fragment (from 0.05 to 0.01 pmol/μl). The final injection solution was filtered through Millipore centrifugal columns and spun at 20,000*g* for 10 min at room temperature.

Microinjections were performed in B6D2F1 (hybrid between C57BL/6J and DBA strains) fertilized one-cell oocytes. Oocytes were removed from oviducts of superovulated B6D2F1 female mice in M2 media supplemented with hyaluronidase (400 μg/ml), washed twice for removal of cumulus cells in M2 media, transferred to KSOM media, and kept at 5% CO_2 and 37°C before injection. Cytoplasmic microinjections were performed in M2 media using the Transjector 5246 (Eppendorf), and Narishige NT-88NE micromanipulators attached to a Nikon Diaphot 300 inverted microscope. Oocytes that survived microinjections were transferred to oviducts of pseudopregnant CD1 foster mice and carried to term. Positively targeted F0 animals were identified by PCR and Southern blot analysis of genomic DNA isolated from tail biopsies.

Donor DNA template preparation

Donor DNA templates for microinjection (table S3) were synthesized and cloned into pUC57 or pBlueScript vector (Biomatic). dsDNA templates were sequenced and directly digested from the $CsCl_2$ gradient purified plasmid vector using Xho I restriction endonuclease. The resulting donor dsDNA fragments were separated using 1% agarose gel electrophoresis, extracted with 6 M NaI, and stored in double-distilled H_2O (ddH_2O). ssDNA templates were either purchased from IDT or MWG or amplified from the aforementioned plasmid vectors using asymmetric PCR with 500 M excess of one of the primers. PCR amplification was performed in 50-μl reaction volume containing 200 ng of plasmid DNA template, primers (1 and 0.002 pmol/μl) (table S3), 50 U of Taq polymerase, 2 U of Phusion DNA polymerase (NEB), and 0.2 mM deoxynucleoside triphosphates (dNTPs). The resulting ssDNA fragments were separated using 1% agarose gel electrophoresis, extracted with 6 M NaI, and stored in ddH_2O.

PCR analysis of the targeting events for HDR, NHEJ, and multiple copy integration

PCR analysis was performed in 50-μl reaction volume containing 1 μM each gene specific primer (table S3), 5 U of Taq polymerase, 100 ng of genomic DNA, 5% dimethyl sulfoxide, 1 M betaine, and 0,2 mM dNTPs. The resulting DNA amplicons were separated using 1% agarose (1× tris-acetate-EDTA buffer) or 6% (w/v) polyacrylamide gel (1× tris-borate–EDTA buffer) electrophoresis, followed by ethidium bromide staining.

Southern blot DNA analysis

Genomic DNA was obtained from tail biopsies. Tail tissue was lysed in buffer containing 100 mM tris-HCl (pH 8.5), 5 mM EDTA, 0.2% SDS, 200 mM NaCl, and proteinase K (100 μg/ml) (Roche) overnight at 55°C. Genomic DNA was extracted by phenol-chloroform and chloroform, followed by precipitation with 2.5 volumes of isopropanol and washing with 70% ethanol. The DNA pellet was dissolved in TE buffer [10 mM tris (pH 7.9) and 0.2 mM EDTA]. Positively targeted F1 animals were analyzed using Southern blot hybridization. Approximately 10 to 20 μg of genomic DNA was digested with the corresponding restriction endonuclease, fractionated on 0.8% agarose gels, and transferred to GeneScreen nylon membranes (NEN DuPont). The membranes were hybridized with ^{32}P-labeled specific DNA probes (table S2). DNA labeling was performed using a random prime DNA labeling kit (Roche) and [α-^{32}P] deoxycytidine-5′ triphosphate (PerkinElmer). Membranes were washed with 0.5× saline sodium phosphate EDTA (SSPE) buffer [1× saline sodium phosphate EDTA buffer is 0.18 M NaCl, 10 mM NaH_2PO_4, and 1 mM EDTA (pH 7.7)] and 0.5% SDS at 65°C and exposed to MS film (Kodak) at −80°C.

Mice

All animal procedures were performed in compliance with the guidelines for the welfare of experimental animals issued by the Federal Government of Germany. F1 heterozygous mice were produced by breeding F0 DBAxC57BL/6J founders to C57BL/6J mice.

Pups were weaned at 19 to 23 days after birth, and females were kept separately from males. The mice were housed in standard individually ventilated cages. General health checks were performed regularly to ensure that any findings were not the result of deteriorating physical conditions of the animals.

SUPPLEMENTARY MATERIALS

Supplementary material for this article is available at http://advances.sciencemag.org/cgi/content/full/6/7/eaax2941/DC1

Supplementary Material and Methods

Fig. S1. Evaluation of in vivo *S100a8* crRNA cleaving efficiency in mouse embryos.

Fig. S2. PCR analysis of genomic DNA from F0 founder number 6 after HTTP integration in the *S100a8* locus at different touch down/annealing temperature conditions using primer pair (d4/r4) (Fig. 1D).

Fig. S3. Sequence analysis of heterozygous animal (F1) number 45 with MC head to tail integration of the DNA template in the *S100a8* gene (Figs. 1E and 2A).

Fig. S4. Analysis of the *Inf2* targeted locus.

Fig. S5. Analysis of the *Trek1* targeted locus.

Fig. S6. Analysis of the *Trpc6* targeted locus.

Fig. S7. Analysis of the *Ccnd2* targeted locus.

Table S1. List of crRNAs used.

Table S2. Designed donor DNA templates.

Table S3. List of oligonucleotides used for ssDNA donor template generation by asymmetric PCR and PCR analyses of targeted loci.

View/request a protocol for this paper from *Bio-protocol*.

REFERENCES AND NOTES

1. A. M. Geurts, G. J. Cost, Y. Freyvert, B. Zeitler, J. C. Miller, V. M. Choi, S. S. Jenkins, A. Wood, X. Cui, X. Meng, A. Vincent, S. Lam, M. Michalkiewicz, R. Schilling, J. Foeckler, S. Kalloway, H. Weiler, S. Ménoret, I. Anegon, G. D. Davis, L. Zhang, E. J. Rebar, P. D. Gregory, F. D. Urnov, H. J. Jacob, R. Buelow, Knockout rats via embryo microinjection of zinc-finger nucleases. *Science* **325**, 433 (2009).
2. J. C. Miller, S. Tan, G. Qiao, K. A. Barlow, J. Wang, D. F. Xia, X. Meng, D. E. Paschon, E. Leung, S. J. Hinkley, G. P. Dulay, K. L. Hua, I. Ankoudinova, G. J. Cost, F. D. Urnov, H. S. Zhang, M. C. Holmes, L. Zhang, P. D. Gregory, E. J. Rebar, A TALE nuclease architecture for efficient genome editing. *Nat. Biotechnol.* **29**, 143–148 (2011).
3. L. Cong, F. A. Ran, D. Cox, S. Lin, R. Barretto, N. Habib, P. D. Hsu, X. Wu, W. Jiang, L. A. Marraffini, F. Zhang, Multiplex genome engineering using CRISPR-Cas systems. *Science* **339**, 819–823 (2013).
4. P. Mali, L. Yang, K. M. Esvelt, J. Aach, M. Guell, J. E. DiCarlo, J. E. Norville, G. M. Church, RNA-guided human genome engineering via Cas9. *Science* **339**, 823–826 (2013).
5. T.-H. Tang, J.-P. Bachellerie, T. Rozhdestvensky, M.-L. Bortolin, H. Huber, M. Drungowski, T. Elge, J. Brosius, A. Hüttenhofer, Identification of 86 candidates for small non-messenger RNAs from the archaeon *Archaeoglobus fulgidus*. *Proc. Natl. Acad. Sci. U.S.A.* **99**, 7536–7541 (2002).
6. F. J. M. Mojica, L. Montoliu, On the origin of CRISPR-Cas technology: From prokaryotes to mammals. *Trends Microbiol.* **24**, 811–820 (2016).
7. E. Deltcheva, K. Chylinski, C. M. Sharma, K. Gonzales, Y. Chao, Z. A. Pirzada, M. R. Eckert, J. Vogel, E. Charpentier, CRISPR RNA maturation by trans-encoded small RNA and host factor RNase III. *Nature* **471**, 602–607 (2011).
8. J. A. Doudna, E. Charpentier, The new frontier of genome engineering with CRISPR-Cas9. *Science* **346**, 1258096 (2014).
9. M. Jinek, K. Chylinski, I. Fonfara, M. Hauer, J. A. Doudna, E. Charpentier, A programmable dual-RNA–guided DNA endonuclease in adaptive bacterial immunity. *Science* **337**, 816–821 (2012).
10. F. Jiang, D. W. Taylor, J. S. Chen, J. E. Kornfeld, K. Zhou, A. J. Thompson, E. Nogales, J. A. Doudna, Structures of a CRISPR-Cas9 R-loop complex primed for DNA cleavage. *Science* **351**, 867–871 (2016).
11. M. D. Canny, N. Moatti, L. C. K. Wan, A. Fradet-Turcotte, D. Krasner, P. A. Mateos-Gomez, M. Zimmermann, A. Orthwein, Y.-C. Juang, W. Zhang, S. M. Noordermeer, E. Seclen, M. D. Wilson, A. Vorobyov, M. Munro, A. Ernst, T. F. Ng, T. Cho, P. M. Cannon, S. S. Sidhu, F. Sicheri, D. Durocher, Inhibition of 53BP1 favors homology-dependent DNA repair and increases CRISPR–Cas9 genome-editing efficiency. *Nat. Biotechnol.* **36**, 95–102 (2018).
12. B. P. Kleinstiver, V. Pattanayak, M. S. Prew, S. Q. Tsai, N. T. Nguyen, Z. Zheng, J. K. Joung, High-fidelity CRISPR–Cas9 nucleases with no detectable genome-wide off-target effects. *Nature* **529**, 490–495 (2016).
13. X.-L. Li, G.-H. Li, J. Fu, Y.-W. Fu, L. Zhang, W. Chen, C. Arakaki, J.-P. Zhang, W. Wen, M. Zhao, W. V. Chen, G. D. Botimer, D. Baylink, L. Aranda, H. Choi, R. Bechar, P. Talbot, C.-K. Sun, T. Cheng, X.-B. Zhang, Highly efficient genome editing via CRISPR–Cas9 in human pluripotent stem cells is achieved by transient BCL-XL overexpression. *Nucleic Acids Res.* **46**, 10195–10215 (2018).
14. C. D. Richardson, G. J. Ray, M. A. DeWitt, G. L. Curie, J. E. Corn, Enhancing homology-directed genome editing by catalytically active and inactive CRISPR-Cas9 using asymmetric donor DNA. *Nat. Biotechnol.* **34**, 339–344 (2016).
15. S. Shao, C. Ren, Z. Liu, Y. Bai, Z. Chen, Z. Wei, X. Wang, Z. Zhang, K. Xu, Enhancing CRISPR/Cas9-mediated homology-directed repair in mammalian cells by expressing *Saccharomyces cerevisiae* Rad52. *Int. J. Biochem. Cell Biol.* **92**, 43–52 (2017).
16. I. M. Slaymaker, L. Gao, B. Zetsche, D. A. Scott, W. X. Yan, F. Zhang, Rationally engineered Cas9 nucleases with improved specificity. *Science* **351**, 84–88 (2016).
17. S. Q. Tsai, J. K. Joung, Defining and improving the genome-wide specificities of CRISPR–Cas9 nucleases. *Nat. Rev. Genet.* **17**, 300–312 (2016).
18. D. Yang, M. A. Scavuzzo, J. Chmielowiec, R. Sharp, A. Bajic, M. Borowiak, Enrichment of G2/M cell cycle phase in human pluripotent stem cells enhances HDR-mediated gene repair with customizable endonucleases. *Sci. Rep.* **6**, 21264 (2016).
19. H. Yin, C.-Q. Song, S. Suresh, S.-Y. Kwan, Q. Wu, S. Walsh, J. Ding, R. L. Bogorad, L. J. Zhu, S. A. Wolfe, V. Koteliansky, W. Xue, R. Langer, D. G. Anderson, Partial DNA-guided Cas9 enables genome editing with reduced off-target activity. *Nat. Chem. Biol.* **14**, 311–316 (2018).
20. W. T. Hendriks, C. R. Warren, C. A. Cowan, Genome editing in human pluripotent stem cells: Approaches, pitfalls, and solutions. *Cell Stem Cell* **18**, 53–65 (2016).
21. R. Peng, G. Lin, J. Li, Potential pitfalls of CRISPR/Cas9-mediated genome editing. *FEBS J.* **283**, 1218–1231 (2016).
22. H. Yang, H. Wang, C. S. Shivalila, A. W. Cheng, L. Shi, R. Jaenisch, One-step generation of mice carrying reporter and conditional alleles by CRISPR/Cas-mediated genome engineering. *Cell* **154**, 1370–1379 (2013).
23. C. Gurumurthy, R. Quadros, J. Adams Jr, P. Alcaide, S. Ayabe, J. Ballard, S. K. Batra, M.-C. Beauchamp, K. A. Becker, G. Bernas, D. Brough, F. Carrillo-Salinas, R. Dawson, V. DeMambro, J. D'Hont, K. Dibb, J. D. Eudy, L. Gan, J. Gao, A. Gonzales, A. Guntur, H. Guo, D. W. Harms, A. Harrington, K. E. Hentges, N. Humphreys, S. Imai, H. Ishii, M. Iwama, E. Jonasch, M. Karolak, B. Keavney, N.-C. Khin, M. Konno, Y. Kotani, Y. Kunihiro, I. Lakshmanan, C. Larochelle, C. B. Lawrence, L. Li, V. Lindner, X.-D. Liu, G. Lopez-Castejon, A. Loudon, J. Lowe, L. Jerome-Majewska, T. Matsusaka, H. Miura, Y. Miyasaka, B. Morpurgo, K. Motyl, Y.-i. Nabeshima, K. Nakade, T. Nakashiba, K. Nakashima, Y. Obata, S. Ogiwara, M. Ouellet, L. Oxburgh, S. Piltz, I. Pinz, M. P. Ponnusamy, D. Ray, R. J. Redder, C. J. Rosen, N. Ross, M. T. Ruhe, L. Ryzhova, A. M. Salvador, R. Sedlacek, K. Sharma, C. Smith, K. Staes, L. Starrs, F. Sugiyama, S. Takahashi, T. Tanaka, A. Trafford, Y. Uno, L. Vanhoutte, F. Vanrockeghem, B. J. Willis, C. S. Wright, Y. Yamauchi, X. Yi, K. Yoshimi, X. Zhang, Y. Zhang, M. Ohtsuka, S. Das, D. J. Garry, T. Hochepied, P. Thomas, J. Parker-Thornburg, A. D. Adamson, A. Yoshiki, J.-F. Schmouth, A. Golovko, W. R. Thompson, KC. Kent Lloyd, J. A. Wood, M. Cowan, T. Mashimo, S. Mizuno, H. Zhu, P. Kasparek, L. Liaw, J. M. Miano, G. Burgio, Re-evaluating one-step generation of mice carrying conditional alleles by CRISPR-Cas9-mediated genome editing technology. bioRxiv 393231 [Preprint].2018. https://doi.org/10.1101/393231.
24. Y. Miyasaka, Y. Uno, K. Yoshimi, Y. Kunihiro, T. Yoshimura, T. Tanaka, H. Ishikubo, Y. Hiraoka, N. Takemoto, T. Tanaka, Y. Ooguchi, P. Skehel, T. Aida, J. Takeda, T. Mashimo, CLICK: One-step generation of conditional knockout mice. *BMC Genomics* **19**, 318 (2018).
25. R. M. Quadros, H. Miura, D. W. Harms, H. Akatsuka, T. Sato, T. Aida, R. Redder, G. P. Richardson, Y. Inagaki, D. Sakai, S. M. Buckley, P. Seshacharyulu, S. K. Batra, M. A. Behlke, S. A. Zeiner, A. M. Jacobi, Y. Izu, W. B. Thoreson, L. D. Urness, S. L. Mansour, M. Ohtsuka, C. B. Gurumurthy, Easi-CRISPR: A robust method for one-step generation of mice carrying conditional and insertion alleles using long ssDNA donors and CRISPR ribonucleoproteins. *Genome Biol.* **18**, 92 (2017).
26. X. Yao, M. Zhang, X. Wang, W. Ying, X. Hu, P. Dai, F. Meng, L. Shi, Y. Sun, N. Yao, W. Zhong, Y. Li, K. Wu, W. Li, Z. J. Chen, H. Yang, Tild-CRISPR allows for efficient and precise gene knockin in mouse and human cells. *Dev. Cell* **45**, 526–536 e5 (2018).
27. M. Adli, The CRISPR tool kit for genome editing and beyond. *Nat. Commun.* **9**, 1911 (2018).
28. G. Gasiunas, R. Barrangou, P. Horvath, V. Siksnys, Cas9–crRNA ribonucleoprotein complex mediates specific DNA cleavage for adaptive immunity in bacteria. *Proc. Natl. Acad. Sci. U.S.A.* **109**, E2579–E2586 (2012).
29. W. Jiang, D. Bikard, D. Cox, F. Zhang, L. A. Marraffini, RNA-guided editing of bacterial genomes using CRISPR-Cas systems. *Nat. Biotechnol.* **31**, 233–239 (2013).
30. S. L. Dallas, Y. Xie, L. A. Shiflett, Y. Ueki, Mouse cre models for the study of bone diseases. *Curr. Osteoporos. Rep.* **16**, 466–477 (2018).
31. C.-X. Deng, Conditional knockout mouse models of cancer. *Cold Spring Harb. Protoc.* **2014**, 1217–1233 (2014).
32. M. P. Parker, K. R. Peterson, Mouse models of erythropoiesis and associated diseases. *Methods Mol. Biol.* **1698**, 37–65 (2018).
33. T. S. Rozhdestvensky, T. Robeck, C. R. Galiveti, C. A. Raabe, B. Seeger, A. Wolters, L. V. Gubar, J. Brosius, B. V. Skryabin, Maternal transcription of non-protein coding RNAs from the PWS-critical region rescues growth retardation in mice. *Sci. Rep.* **6**, 20398 (2016).
34. B. V. Skryabin, L. V. Gubar, B. Seeger, J. Pfeiffer, S. Handel, T. Robeck, E. Karpova, T. S. Rozhdestvensky, J. Brosius, Deletion of the MBII-85 snoRNA gene cluster in mice results in postnatal growth retardation. *PLOS Genet.* **3**, e235 (2007).
35. K. Rajewsky, H. Gu, R. Kühn, U. A. Betz, W. Müller, J. Roes, F. Schwenk, Conditional gene targeting. *J. Clin. Invest.* **98**, 600–603 (1996).
36. J. Zhang, J. Zhao, W.-j. Jiang, X.-w. Shan, X.-m. Yang, J.-g. Gao, Conditional gene manipulation: Cre-ating a new biological era. *J. Zhejiang Univ. Sci. B* **13**, 511–524 (2012).

Acknowledgments: We thank S. Klco-Brosius for editing assistance. **Funding:** This work was supported by the Deutsche Forschungsgemeinschaft (RO5622/1-1 to T.S.R., SK259/2-1 to B.V.S., SU 195/4-1 to C.S., SFB/CRC 1009-B09 to J.R., and SFB/CRC 1009-B10 to H.P. and R.W.-S.), BMBF (16GW0055 to S.G.M.), DZHK (81X2800174 to B.V.S.), the IZKF Muenster (Wed2/022/18 to R.W.-S.), Cancerfonden (CAN 2016/524 to Y.B.S.), Strategic Research grant from Medical Faculty, Umeå University (to Y.B.S.), and an IMF grant of the Medical Faculty of WWU (SH121608 to J.S.). Core Facility TRAM is an institution of the Medical Faculty of WWU. The support of the Medical Faculty is thankfully recognized. **Competing interests:** The authors declare that they have no competing interests. **Author contributions:** B.V.S. and T.S.R. conceived and designed the study. L.G., B.S., H.K., A.S., B.V.S., and T.S.R. were involved in experimental work for all cKO projects. D.-M.K. cloned and analyzed junction sites of repeats. J.R., S.G.M., Y.B.S., and C.S. were involved in the generation of *S100a8*, *Trek1*, *Ccnd2*, and *Il4* cKO mice, respectively. H.P. and R.W.-S. participated in the *Inf2* cKO project. J.S. and T.P. were involved in *Trpc6* cKO mice generation. T.S.R., B.V.S., and J.B. analyzed the data and wrote the paper. All authors provided input and approved the final manuscript. **Data and materials availability:** All data needed to evaluate the conclusions in the paper are present in the paper and/or the Supplementary Materials. Additional data related to this paper may be requested from the authors.

Submitted 11 March 2019
Accepted 25 November 2019
Published 12 February 2020
10.1126/sciadv.aax2941

Citation: B. V. Skryabin, D.-M. Kummerfeld, L. Gubar, B. Seeger, H. Kaiser, A. Stegemann, J. Roth, S. G. Meuth, H. Pavenstädt, J. Sherwood, T. Pap, R. Wedlich-Söldner, C. Sunderkötter, Y. B. Schwartz, J. Brosius, T. S. Rozhdestvensky, Pervasive head-to-tail insertions of DNA templates mask desired CRISPR-Cas9–mediated genome editing events. *Sci. Adv.* **6**, eaax2941 (2020).